European Radiology (2019) 29:3647–3657
https://doi.org/10.1007/s00330-019-06139-2

CARDIAC

The best predictor of ischemic coronary stenosis: subtended myocardial volume, machine learning–based FFR_{CT}, or high-risk plaque features?

Mengmeng Yu[1] · Zhigang Lu[2] · Chengxing Shen[2] · Jing Yan[3] · Yining Wang[4] · Bin Lu[5] · Jiayin Zhang[1]

Received: 3 January 2019 / Revised: 16 February 2019 / Accepted: 7 March 2019 / Published online: 22 March 2019

Abstract

Objectives The present study aimed to compare the diagnostic performance of a machine learning (ML)–based FFR_{CT} algorithm, quantified subtended myocardial volume, and high-risk plaque features for predicting if a coronary stenosis is hemodynamically significant, with reference to FFR_{ICA}.

Methods Patients who underwent both CCTA and FFR_{ICA} measurement within 2 weeks were retrospectively included. ML-based FFR_{CT}, volume of subtended myocardium (V_{sub}), percentage of subtended myocardium volume versus total myocardium volume (V_{ratio}), high-risk plaque features, minimal lumen diameter (MLD), and minimal lumen area (MLA) along with other parameters were recorded. Lesions with $FFR_{ICA} \leq 0.8$ were considered to be functionally significant.

Results One hundred eighty patients with 208 lesions were included. The lesion length (LL), diameter stenosis, area stenosis, plaque burden, V_{sub}, V_{ratio}, V_{ratio}/MLD, V_{ratio}/MLA, and LL/MLD^4 were all significantly longer or larger in the group of $FFR_{ICA} \leq 0.8$ while smaller minimal lumen area, MLD, and FFR_{CT} value were noted. The AUC of $FFR_{CT} + V_{ratio}$/MLD was significantly better than that of FFR_{CT} alone (0.935 versus 0.873, $p < 0.001$). High-risk plaque features failed to show difference between functionally significant and insignificant groups. V_{ratio}/MLD-complemented ML-based FFR_{CT} for "gray zone" lesions with FFR_{CT} value ranged from 0.7 to 0.8 and the combined use of these two parameters yielded the best diagnostic performance (86.5%, 180/208).

Conclusions ML-based FFR_{CT} simulation and V_{ratio}/MLD both provide incremental value over CCTA-derived diameter stenosis and high-risk plaque features for predicting hemodynamically significant lesions. V_{ratio}/MLD is more accurate than ML-based FFR_{CT} for lesions with simulated FFR_{CT} value from 0.7 to 0.8.

Key Points

- *Machine learning–based FFR_{CT} and subtended myocardium volume both performed well for predicting hemodynamically significant coronary stenosis.*
- *Subtended myocardium volume was more accurate than machine learning–based FFR_{CT} for "gray zone" lesions with simulated FFR value from 0.7 to 0.8.*
- *CT-derived high-risk plaque features failed to correctly identify hemodynamically significant stenosis.*

Mengmeng Yu and Zhigang Lu contributed equally to this work.

Electronic supplementary material The online version of this article (https://doi.org/10.1007/s00330-019-06139-2) contains supplementary material, which is available to authorized users.

✉ Jiayin Zhang
andrewssmu@msn.com

[1] Institute of Diagnostic and Interventional Radiology, Shanghai Jiao Tong University Affiliated Sixth People's Hospital, #600, Yishan Rd, Shanghai 200233, China

[2] Department of Cardiology, Shanghai Jiao Tong University Affiliated Sixth People's Hospital, #600, Yishan Rd, Shanghai, China

[3] Siemens Healthineers, #278, Zhouzhugong Rd, Shanghai, China

[4] Department of Radiology, Peking Union Medical College Hospital, Chinese Academy of Medical Science & Peking Union Medical College, Beijing, China

[5] Department of Radiology, Fuwai Hospital, State Key Laboratory of Cardiovascular Disease, National Centre for Cardiovascular Diseases, Chinese Academy of Medical Sciences and Peking Union Medical College, Beijing, China

Keywords Coronary artery disease · Multidetector computed tomography · Angiography · Myocardial fractional flow reserve · Percutaneous coronary intervention

Abbreviations

AUC	Area under the curve
CCTA	Coronary computed tomography angiography
CFD	Computational fluid dynamics
DJS	Duke Jeopardy Score
FFR	Fractional flow reserve
ICA	Invasive coronary angiography
LL	Lesion length
ML	Machine learning
MLA	Minimal lumen area
MLD	Minimal lumen diameter
ROC	Receiver operating characteristic

Introduction

Coronary computed tomography angiography (CCTA) is an accurate imaging modality for ruling out obstructive coronary artery disease (CAD) when compared with invasive coronary angiography (ICA) [1–3]. However, these anatomy-based imaging methods lack functional information to determine the hemodynamic significance of coronary stenosis, which is more important for clinical decision-making. In contrast to the above imaging modalities, fractional flow reserve (FFR) is currently the gold standard for the evaluation of functional status of coronary lesions. According to previous large clinical trials, FFR is more favored than ICA for guiding revascularization strategy and leads to better clinical outcomes [4, 5].

Through computational fluid dynamics (CFD), it is possible to calculate FFR_{CT} from standard CCTA [6–8]. However, this method is time-consuming. Recently, machine learning (ML)–based FFR_{CT} has been introduced for differentiating flow-limiting and non-flow-limiting coronary stenosis with very short processing time and with promising preliminary results [9]. CT-derived high-risk plaque features might also be independent predictors of hemodynamic significance regardless of lesion's geometrical features [10, 11]. In addition, Duke Jeopardy Score (DJS) is an angiography-based index to roughly estimate the amount of myocardium subtended by a coronary stenosis [12]. A previous study has shown that the extent of subtended myocardium as evaluated by DJS was a predictor of flow-limiting lesions [13]. With the development of computational technique, it is now technically feasible to use CCTA data to further absolutely quantify the subtended myocardium volume [14]. Consequently, we hypothesized that CT-derived plaque characteristics and absolute myocardial volume quantification might provide incremental values to the ML-based FFR_{CT} method. Therefore, we aimed to investigate the diagnostic performance of ML-based FFR_{CT} method combined with quantified myocardium volume as well as high-risk plaque features for the prediction of hemodynamically significant coronary stenosis.

Materials and methods

Patients' population

The Institutional Review Board of the hospital approved this retrospective study, and the informed consent was waived as well. We retrospectively searched the hospital database from January 2012 to December 2017 to include patients with clinically suspected CAD who underwent both CCTA and invasive coronary angiography (ICA)/FFR measurement. The FFR measurement was clinically indicated to assess the hemodynamic significance of coronary stenosis in order to optimize the treatment strategy (revascularization or medical treatment). The inclusion criterion was the interval between the CCTA examination and FFR_{ICA} measurement within 2 weeks.

The exclusion criteria were as follows: (I) previous history of coronary revascularization; (II) previous history of myocardial infarction; (III) insufficient image quality of CCTA examination; (IV) patients with coronary anomalies or concomitant cardiomyopathy; and (V) the interval between CCTA and FFR measurement was longer than 2 weeks (Fig. 1).

CCTA protocol

A 128-slice multidetector CT (Definition AS+, Siemens Healthineers) was used for data acquisition. In all patients with an initial heart rate of > 65 bpm, 25–75 mg β-blocker (Betaloc ZOK, AstraZeneca) was administrated orally 1 h prior to the examination. Nitroglycerin was administered sublingually in all patients. Retrospective ECG-gated CTA was employed in patients with a final heart rate of ≥ 70 bpm whereas prospective ECG-triggered sequential acquisition was performed in patients with a final heart rate of < 70 bpm. The details of CCTA acquisition were given in online appendix.

Reconstruction and CT-derived plaque analysis

Data were transferred to an offline workstation (Syngo.via, Siemens Healthineers) for reconstruction and post-processing. The image quality was evaluated by using a 4-point Likert

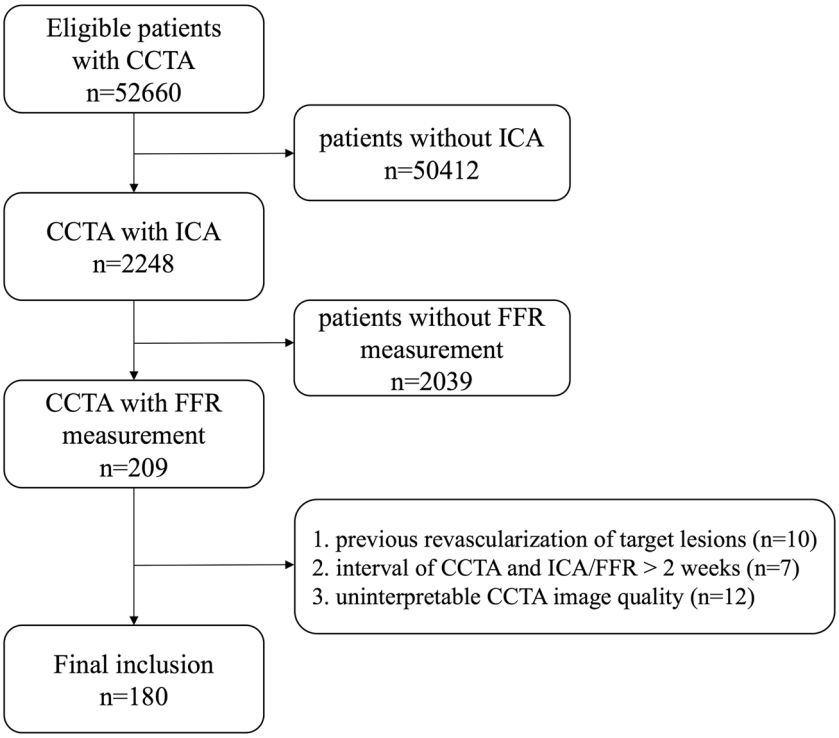

Fig. 1 A flow chart illustrating inclusion and exclusion criteria. CCTA, coronary computed tomography angiography; FFR, fractional flow reserve; ICA, invasive coronary angiography

scale: 4 = excellent (in the absence of artifact), 3 = good (in the presence of mild artifact), 2 = sufficient (in the presence of moderate artifact, but still diagnostic), and 1 = poor (in the presence of severe artifact, non-diagnostic). Only patients with the image quality of grades 3–4 were included for further analysis.

The plaque characterization was performed according to CCTA findings and a series of quantified plaque features were measured by using a dedicated plaque analysis software (Coronary Plaque Analysis, version 2.0, Siemens Healthineers). The recorded parameters were as follow: (1) a remodeling index; (2) low-attenuation plaque (LAP); (3) a spotty calcification; (4) napkin-ring sign (NRS) as defined by previous study [15]; (5) lesion length; (6) plaque volume; (7) plaque burden;(8) the minimal lumen area (MLA) and the minimal lumen diameter (MLD); (9) the diameter stenosis and area stenosis; and (10) DJS. The detailed definitions of the above parameters were given in online appendix.

The amount of perfused myocardium subtended by the target stenosis was quantified according to the concept of the Voronoi algorithm by using a commercially available software (Ziostation, Ziosoft). In brief, the location of each target lesion was manually marked by observers. Then, the algorithm automatically calculated the subtended myocardial volume by aggregating all myocardial voxels connected to the voxels on the coronary arteries that were distal to the target lesion. The volume (V_{sub}) and percentage (V_{ratio}) of the subtended myocardium were consequently generated by the software.

The results of a previous study revealed that the ratio of DJS versus MLD (DJS/MLD) outperformed other combinations of morphological parameters, such as DJS/MLA and the ratio of LL versus the fourth power of MLD (LL/MLD^4), for the prediction of hemodynamically significant lesions [13]. In the present study, we replaced DJS with a more precise parameter, V_{ratio}, to represent the extent of myocardium subtended by coronary stenosis and therefore tested the diagnostic performance of different combinations (V_{ratio}/MLD, V_{ratio}/MLA, and LL/MLD^4).

Two cardiovascular radiologists (with 10 and 8 years of experience on cardiac imaging), who were blinded to ICA and FFRICA results, independently analyzed the lesions. The mean values of quantitative parameters measured by two observers were used for further analysis.

FFR_{CT} analysis

A machine learning–based algorithm (cFFR, version 3.0, Siemens Healthineers) was used for FFR_{CT} simulation [9]. This model was trained on a large database of synthesized coronary anatomies, where the reference values are computed using a CFD-based model. For on-site processing, few steps have to be taken manually to determine the vessel centerline, luminal contour, and coronary stenosis before the final computation could be finished [16]. More details regarding the mechanism and processing procedure of this approach are given in online appendix. Two cardiovascular radiologists (with 10 and 8 years of experience on cardiac imaging), who

were blinded to ICA and FFR results, independently performed the FFR_{CT} simulation and the mean values of lesions were used for further analysis.

ICA and FFR measurement

ICA was performed using a standard method and at least two views were obtained for each major coronary artery. The images were independently evaluated by two interventional cardiologists (with 26 and 20 years of experience on coronary intervention), who were blinded to the results of CCTA as well as FFR_{CT}. The stenotic extent of each lesion was recorded according to visual assessment. FFR_{ICA} was clinically indicated to assess the necessity for revascularization. FFR was measured by using a 0.014-in. pressure guidewire (St Jude Medical) as previously described [17]. Hyperemia was induced by intravenous infusion of adenosine at the dose of 140 μg per kilogram of body weight per minute. Besides, FFR $\leq$ 0.8 was considered physiologically significant stenosis.

Statistical analysis

Statistical analysis was performed by using a commercial statistical software (MedCalc Statistical Software, version 15.2.2; MedCalc Software bvba). One-sample Kolmogorov-Smirnov test was used to check the assumption of normal distribution. Normally distributed continuous quantitative variables were expressed as mean ± standard deviation (SD), or median with first to third quartiles. Student's *t* test was used for normally distributed data, and the Mann-Whitney *U* test was used for the data that were not normally distributed. Categorical variables were reported as count (%) and compared by the Fisher's exact test or chi-square test, according to the data cell size. Intra-observer and inter-observer agreements of all parameters were examined for intra-class correlation coefficients (ICC). All lesions were then classified as functionally significant or functionally non-significant (according to FFR values) for evaluating the association between the respective variables and the hemodynamic relevance of the lesions. The correlations between FFR value and all parameters were assessed by Pearson's correlation coefficient when data were normally distributed or according to Spearman's rank correlation coefficient when data were not normally distributed. The Bland-Altman method was used to plot the difference between FFR_{CT} and FFR_{ICA} versus the average of FFR_{CT} and FFR_{ICA} measurements. Receiver operating characteristic (ROC) curve analyses were performed to calculate the area under the ROC curve (AUC). The optimal cut-off values for various parameters were determined by Youden's index, and the maximum sum of sensitivity and specificity at ROC curve analysis was calculated based on a method developed by DeLong et al [18]. The combined performance of FFR_{CT} with other parameters was investigated using binary logistic regression (details in Online Appendix). In addition, a stepwise approach based on FFR_{CT} with restrictive use of V_{ratio}/MLD was designed. Lesions with FFR_{CT} values within previously reported "gray zone" range (FFR_{CT} value ranging from 0.7 to 0.8) [19] were reclassified according to the results of V_{ratio}/MLD. Sensitivity, specificity, positive predictive value (PPV), negative predictive value (NPV), and

Table 1 Clinical characteristics

Characteristic	Datum
Number of patients	180
Number of lesions	208
Ages (years)[a]	63 ± 7.5
Male	116 (64.4)
Risk factors[b]	
Hypertension	114 (63.3)
Diabetes mellitus	106 (58.9)
Dyslipidemia	96 (53.3)
Current smoker	57 (31.7)
Distribution of lesion[b]	
Left artery descending	118 (56.7)
Right coronary artery	58 (27.9)
Left circumflex artery	22 (10.6)
Diagonal branch	7 (3.4)
Obtuse marginal	2 (0.96)
Posterior descending branch	1 (0.48)
Stenosis extent[b]	
50–69%	98 (47.1)
≥70%	110 (52.9)
CACS [c]	
Patient-based Agatston score	113.6 (11.4–392.3)
Lesion-based Agatston score	26.8 (0–138.2)
Single-vessel disease	150 (87.2)
Multi-vessel disease	22 (12.8)
Non-tandem lesions[b]	181 (92.3)
Tandem lesions[b]	15 (7.7)
Image quality score	
4	125 (69.4)
3	55 (30.6)

Unless otherwise specified, data are numbers of patients with percentages in parentheses

CACS, coronary artery calcification score

[a] Data are mean ± the standard deviation

[b] Data are numbers of lesions, with percentages in parentheses

[c] Data are medians, with first to third quartile in parentheses

Table 2 Comparison of CCTA parameters between hemodynamically significant and non-significant stenosis

	All (n = 208)	FFR ≤ 0.8 (n = 80)	FFR > 0.8 (n = 128)	p value
MLD (mm)	1.39 ± 0.41	1.19 ± 0.30	1.50 ± 0.42	< 0.001
MLA (mm^2)	2.05 ± 0.82	1.61 ± 0.44	2.31 ± 0.86	< 0.001
Diameter stenosis (%)	70.57 ± 10.93	76.30 ± 8.93	67.31 ± 10.65	< 0.001
Area stenosis (%)	76.18 ± 9.56	81.41 ± 8.07	73.55 ± 9.72	< 0.001
Plaque burden (%)	76.40 ± 9.66	80.72 ± 8.07	73.6 ± 9.81	< 0.001
LL (mm)	9.70 ± 3.59	12.54 ± 4.2	8.09 ± 3.02	< 0.001
Low-attenuation plaque	17.4% (36)	19.9% (16)	15.6% (20)	0.509
Napkin-ring sign	20.7% (43)	23.8% (19)	18.8% (24)	0.433
Spotty calcification	4.8% (10)	5.0% (4)	5.5% (7)	1.000
Positive remodeling	36.1% (75)	36.3% (29)	35.9% (46)	0.931
V_{sub} (ml)	29.67 ± 8.91	39.39 ± 10.69	24.14 ± 5.70	< 0.001
V_{ratio} (%)	24.43 ± 8.21	30.36 ± 10.11	21.07 ± 7.57	< 0.001
V_{ratio}/MLD	19.17 ± 7.23	26.46 ± 10.28	15.03 ± 7.43	< 0.001
V_{ratio}/MLA	20.50 ± 8.13	30.72 ± 12.33	14.69 ± 6.89	< 0.001
LL/MLD^4	5.21 ± 1.81	8.43 ± 3.25	3.37 ± 1.22	< 0.001
FFR_{CT}	0.81 ± 0.11	0.71 ± 0.10	0.86 ± 0.08	< 0.001

CCTA, coronary computed tomography angiography; *FFR*, fractional flow reserve; *LL*, lesion length; *MLA*, minimal lumen area; *MLD*, minimal lumen diameter; V_{sub}, volume of subtended myocardial mass; V_{ratio}, percentage of subtended myocardial mass

accuracy were recorded as well. A two-tailed p value < 0.05 was statistically considered significant.

Results

Clinical characteristics

A total of 52,600 patients who underwent CCTA from January 2012 to December 2017 were initially reviewed. Besides, 50,412 patients without ICA and 2039 patients with ICA (but without FFR_{ICA} measurement) were excluded. Seven patients were subsequently excluded because the interval between CCTA and ICA was longer than 2 weeks whereas further exclusion of 12 patients was due to uninterpretable CCTA images. Ten patients with a history of target lesion revascularization were further excluded (Fig. 1).

Eventually, 180 patients (mean age, 63 ± 7.5 years), including 116 males (mean age, 62.1 ± 7.8 years) and 64 females (mean age, 64.2 ± 9.5 years; p = 0.54) with 208 lesions, were included in our study. The mean interval between ICA and CCTA was 7.3 ± 3.5 days. The mean dose length product of CCTA was 510.7 ± 102.6 mGy cm and mean effective dose was 7.6 ± 1.8 mSv. Detailed demographic data are given in Table 1. The average processing time for FFR_{CT} calculation and CT-based myocardium quantification was 7.1 ± 2.8 and 10.2 ± 3.1 min, respectively.

Correlation of CCTA-derived morphological parameters and FFR_{CT} with functionally significant stenosis (FFR ≤ 0.8)

Lesions were divided into two subgroups for further analysis, by using a FFR value of 0.8 as a cut-off. Stenosis morphology as evaluated by CCTA, diameter stenosis, area stenosis, plaque burden, total lesion length, V_{sub}, V_{ratio}, V_{ratio}/MLD, V_{ratio}/MLA, and LL/MLD^4 were all significantly longer or larger in the group of hemodynamic significant lesions (FFR ≤ 0.8, p < 0.05) compared with the group of insignificant lesions (FFR > 0.8) (for all p < 0.001), as shown in Table 2. In addition, smaller MLD, MLA, and FFR_{CT} were associated with functionally significant lesions (1.19 ± 0.30 vs. 1.50 ± 0.42; 1.61 ± 0.44 vs. 2.31 ± 0.86; 0.71 ± 0.10 vs. 0.86 ± 0.08, respectively; for all p < 0.001) (Figs. 2 and 3). However, there were no significant differences between the hemodynamic significant subgroup and the insignificant subgroup with respect to the risky plaque features as evaluated at CCTA (low-attenuation plaque, spotty calcification, napkin-ring sign, positive remodeling) (for all p > 0.05).

Pearson correlation analysis demonstrated that the FFR_{CT}, V_{ratio}/MLD, and V_{ratio}/MLA all correlated well with the FFR_{ICA} value (r = 0.72, − 0.62, and − 0.6, respectively; for all p < 0.001), whereas other parameters showed a poor correlation (Online Supplement Table E1). FFR_{CT} showed a slight underestimation compared with FFR_{ICA} (Fig. 4). The intra-

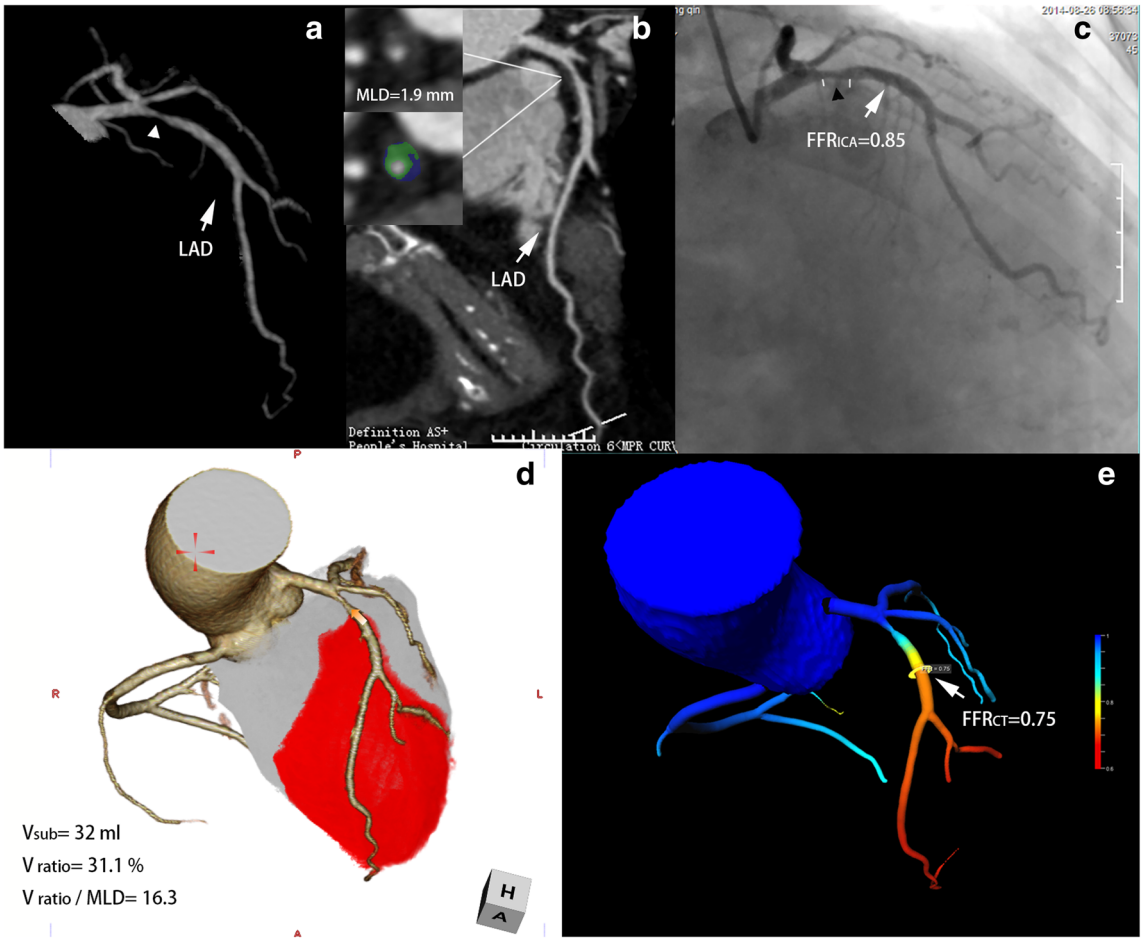

Fig. 2 CCTA evaluation of severe coronary stenosis with an FFR of more than 0.8. **a** Three-dimensional MIP showed a severe coronary stenosis (white arrowhead) in the proximal LAD. **b** CPR showed the severe stenosis with non-calcified plaque at proximal LAD. The cross-section imaging revealed that the MLD was 1.9 mm. NRS and LAP were present as the color-coded plaque analysis showing low-density plaque component (< 30 HU, blue area) within the plaque. **c** ICA showed severe stenosis located at the proximal LAD with an FFR value of 0.85. **d** Left ventricle quantification demonstrated that the volume and percentage of subtended myocardium was 32 ml and 31.1%, respectively. The V_{ratio}/MLD was 16.3, which was less than the best cut-off value and indicated hemodynamically insignificant of coronary stenosis. **e** FFR_{CT} revealed that the LAD lesion had a simulated FFR value of 0.75, which was mismatched with FFR_{ICA}. CCTA, coronary computed tomography angiography; CPR, curved planar reformation; FFR, fractional flow reserve; ICA, invasive coronary angiography; LAD, left anterior descending; LAP, low-attenuation plaque; LL, lesion length; MIP, maximum intensity projection; MLD, minimal lumen diameter; NRS, napkin-ring sign

observer and inter-observer agreements of all parameters are shown in Online Supplement Tables E2–3.

Diagnostic performance of CCTA-derived parameters and FFR_{CT} for the prediction of functionally significant coronary stenosis (FFR ≤ 0.8)

For single parameters, according to ROC curve analysis, the FFR_{CT} showed the largest AUC (AUC = 0.873, 95%CI = 0.820–0.915) for diagnosing functionally significant stenosis (Table 3, Fig. 5). V_{ratio}/MLD (AUC = 0.854, 95%CI = 0.799–0.899) and V_{ratio}/MLA (AUC = 0.839, 95%CI = 0.781–0.886) had a similar diagnostic performance compared with FFR_{CT}, whereas other parameters were less accurate (Table 3). For combined analysis, FFR_{CT} + V_{ratio}/MLD was revealed to have the significant larger AUC (AUC = 0.935, 95%CI = 0.892–0.964) than any other parameters (Table 3). More specifically, the AUC of FFR_{CT} combined with V_{ratio}/MLD was significantly better than that of FFR_{CT} alone (0.935 vs. 0.873, p = 0.0068).

The overall diagnostic accuracy of FFR_{CT} analysis was 81.2% (Table 4). However, the diagnostic accuracy of FFR_{CT} markedly varied for vessels with FFR_{CT} values below 0.70, 0.70 to 0.79, 0.80, and 0.89, and above 0.89 (see Table 5). In our cohort, 55 lesions (26.4%) had FFR_{CT} values between 0.70 and 0.79. Among them, only 34 lesions were truly within that range as determined by FFR_{ICA}. The diagnostic accuracy of those "gray zone" FFR_{CT} lesions (61.8%, 34/55) could be significantly improved to 80% (44/55) (p = 0.0001), if these lesions were evaluated with V_{ratio}/ MLD

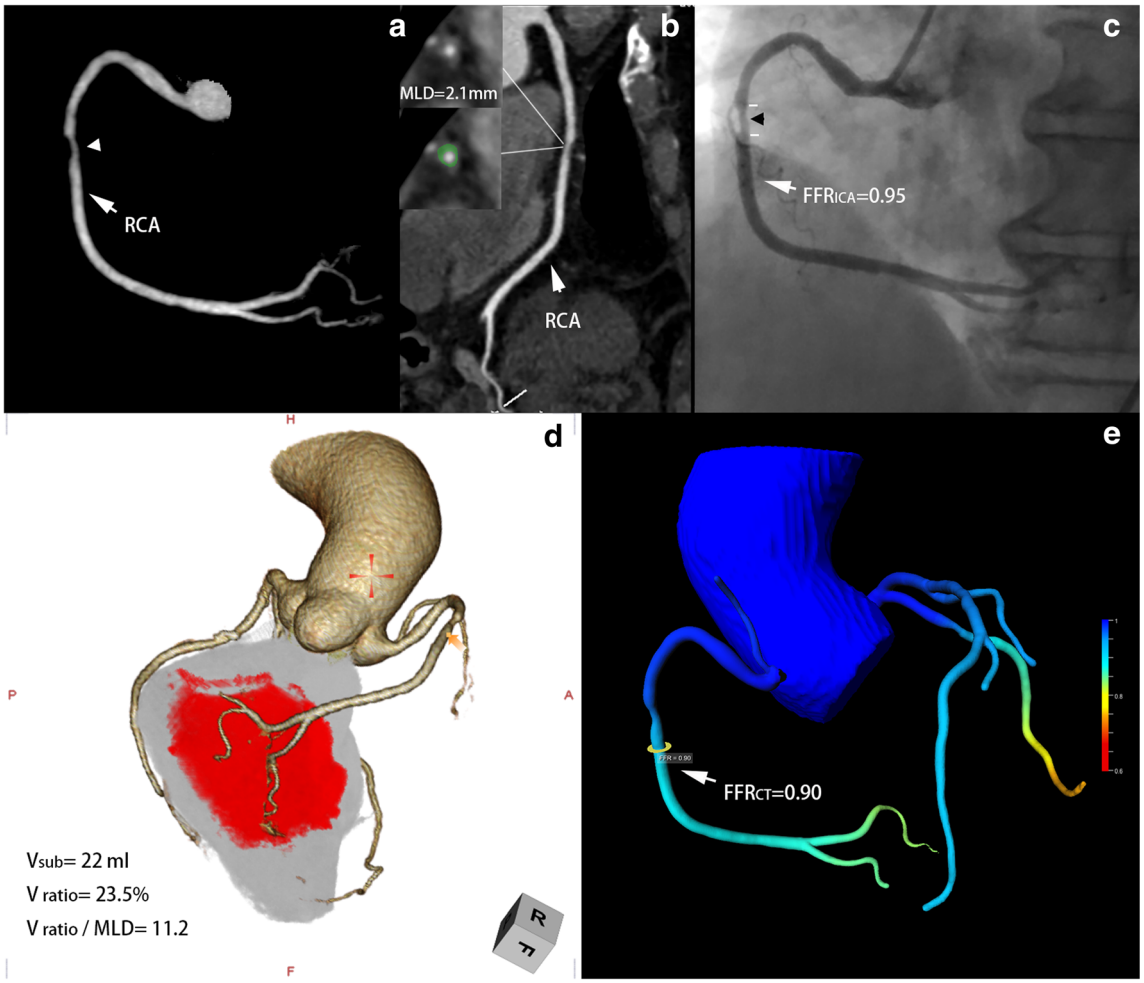

Fig. 3 CCTA evaluation of moderate coronary stenosis with an FFR of greater than 0.8. **a** Three-dimensional MIP images showed moderate coronary stenosis (white arrowhead) in the middle RCA. **b** CPR revealed moderate stenosis with non-calcified plaque at the middle RCA. The cross-sectional imaging demonstrated that the MLD was 2.1 mm. High-risk plaque features were absent according to plaque analysis. **c** ICA showed moderate stenosis located at the middle RCA with an FFR value of 0.95. **d** Left ventricle quantification demonstrated that the volume and percentage of subtended myocardium were 22 ml and 23.5%, respectively. The V_{ratio}/MLD was 11.2, which was less than the best cut-off value and indicated hemodynamically insignificant coronary stenosis. **e** FFR_{CT} revealed that the LAD lesion had a simulated FFR value of 0.9, which was in accordance with FFR_{ICA}. CCTA, coronary computed tomography angiography; CPR, curved planar reformation; FFR, fractional flow reserve; ICA, invasive coronary angiography; LL, lesion length; MIP, maximum intensity projection; MLD, minimal lumen diameter; RCA, right coronary artery

instead of FFR_{CT}. For the total 208 lesions, this stepwise approach correctly classified 189 lesions and provided incremental diagnostic accuracy over FFR_{CT} or V_{ratio}/ MLD alone (90.9% [189/208] vs. 82.7% [172/208]; 90.9% [189/208] vs. 80.3% [167/208]).

Discussion

The major finding of the present study is that ML-based FFR_{CT} simulation and V_{ratio}/MLD both performed well for the prediction of hemodynamic status. V_{ratio}/MLD was more accurate than ML-based FFR_{CT} for lesions with simulated FFR value ranging from 0.7 to 0.8. However, the high-risk plaque features failed to show significant correlation with the hemodynamic significance.

FFR-guided revascularization strategy is associated with better clinical outcomes as well as less unnecessary percutaneous coronary intervention procedures [20–22]. Recently, a ML-based FFR_{CT} approach was developed as a method for non-invasive evaluation of the hemodynamic status of coronary stenosis. It enabled simulation of FFR value from a standard CCTA scanning at a remarkably shorter processing time compared with a CFD-based approach [9]. Despite its promising role, previous studies identified "gray zone" lesions, corresponding to FFR_{CT} values ranging between 0.7 and 0.8: according to a meta-analysis, the diagnostic accuracy was only 46.1% for CFD-based FFR_{CT} in such cases [19]. Our study had similar findings for ML-based FFR_{CT}, showing excellent

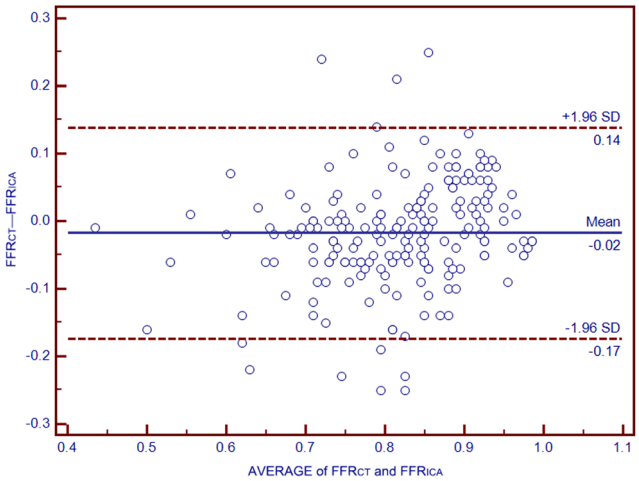

Fig. 4 Bland-Altman plot showed that the mean difference between FFR_{CT} and FFR_{ICA} was − 0.02. A line is placed at the mean difference value (− 0.02) and the corresponding double standard deviation intervals (− 0.17 and 0.14)

diagnostic performance when the simulated value was below 0.7 or above 0.8, and only 61.8% between 0.7 and 0.8.

Interestingly, we found that the addition of V_{ratio}/MLD to ML-based FFR_{CT} improved the diagnostic accuracy from 61.8 to 80% for the "gray zone" lesions. Our previous study validated the diagnostic value of using DJS based on a CT morphological index for discrimination of flow-limiting and non-flow-limiting lesions [13]. However, DJS can only approximately evaluate the stenosis-subtended myocardial volume. In addition, the value of the index is limited when a coronary anomaly is present or major side branch vessels are absent. In the current study, we replaced DJS with absolute quantification of myocardial volume. A large myocardial volume was associated with significant inducible ischemia even with the same degree of stenosis [23]. Thus, the addition of absolute quantification of myocardial volume to anatomical stenosis may reduce the misdiagnosis of ischemic coronary stenosis with reference to FFR_{ICA}. Therefore, the potential clinical implication lies in the combined use of these parameters for more accurate functional assessment of coronary stenosis. In other words, for lesions with FFR_{CT} values less than 0.7 or more than 0.8, ML-based FFR_{CT} is an accurate approach with very high negative predictive value to safely rule out hemodynamically significant lesions and avoid unnecessary invasive procedures. For lesions with FFR_{CT} values between 0.7 and 0.8, V_{ratio}/MLD performed better than ML-based FFR_{CT} and combined use of the above parameters would be recommended.

High-risk plaque features evaluated by CCTA were found to be irrelevant to the hemodynamic significance of coronary stenosis in our study. Discrepant results have been reported according to previous studies regarding the association between plaque histology and hemodynamic significance [24–27]. There were CCTA studies showing that the presence of a large necrotic core as well as the total LAP volume may contribute to the hemodynamic significance of coronary stenosis [24, 25]. In contrast, our results are more in line with other intravascular ultrasound studies that there was no association between plaque composition and FFR value [26, 27]. We found that the geometrical features, such as lesion length, entrance angle, exit angle, size of the reference vessel, and

Table 3 ROC analysis for discriminating hemodynamically significant and non-significant stenosis

	AUC	Best cut-off value	95%CI	*p* value*
MLD (mm)	0.740	≤ 1.4	0.679–0.802	< 0.001
MLA (mm^2)	0.730	≤ 1.95	0.664–0.789	< 0.001
Diameter stenosis (%)	0.750	> 70.53	0.689–0.810	< 0.001
Area stenosis (%)	0.750	> 76.92	0.688–0.810	< 0.001
Plaque burden (%)	0.737	> 77.92	0.672–0.796	< 0.001
Lesion length (mm)	0.653	> 10.6	0.583–0.717	0.0003
V_{sub} (ml)	0.695	> 29.0	0.627–0.757	< 0.001
V_{ratio} (%)	0.772	> 24.5	0.709–0.827	< 0.001
V_{ratio}/MLD	0.854	> 19.6	0.799–0.899	< 0.001
V_{ratio}/MLA	0.839	> 26.625	0.781–0.886	< 0.001
LL/MLD^4	0.793	> 3.067	0.731–0.846	< 0.001
FFR_{CT}	0.873	≤ 0.79	0.820–0.915	< 0.001
FFR_{CT} + V_{ratio}/MLD	0.935	> 0.2678	0.892–0.964	< 0.001
FFR_{CT} + V_{ratio}/MLA	0.914	> 0.3905	0.867–0.948	< 0.001
FFR_{CT} + LL/MLD^4	0.895	> 0.3808	0.845–0.933	< 0.001

AUC, area under curve; *CI*, confidence interval; *FFR*, fractional flow reserve; *LL*, lesion length; *MLA*, minimal lumen area; *MLD*, minimal lumen diameter; *ROC*, receiver operating curve; V_{sub}, volume of subtended myocardial mass; V_{ratio}, percentage of subtended myocardial mass

*Refers to the *p* value of AUCs

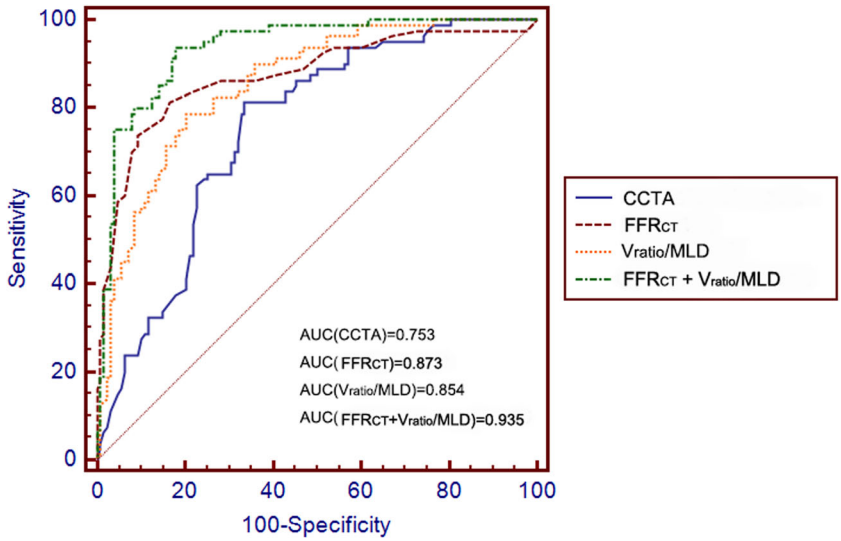

Fig. 5 ROC curve analysis of FFR_{CT}, V_{ratio}/MLD, and combined FFR_{CT} + V_{ratio}/MLD for the identification of functionally significant coronary stenosis. FFR_{CT} + V_{ratio}/MLD showed significant improvement over CCTA, FFR_{CT}, or V_{ratio}/MLD merely for diagnosing flow-limiting coronary stenosis. *FFR_{CT} + V_{ratio}/MLD had the largest AUC compared with other parameters (all $p < 0.05$). FFR_{CT} and V_{ratio}/MLD had similar AUC ($p = 0.6204$). AUC, area under curve; CCTA, coronary computed tomography angiography; FFR, fractional flow reserve; MLD, minimal lumen diameter; ROC, receiver operating characteristic

absolute blood flow relative to the territory supplied of coronary lesions, are more important factors than high-risk plaque features to affect the downstream myocardial perfusion. In contrast, high-risk plaque features are more likely to be linked to the risk of cardiac events [28–30]. Therefore, it seems reasonable to estimate that lesions with similar geometrical features and different plaque compositions tend to have comparable hemodynamic significance but heterogeneous prognosis.

The current study used a commercially available software to quantify the myocardial volume subtended by coronary stenosis. This technique is theoretically based on the concept

Table 4 Diagnostic performance of CCTA parameters for predicting hemodynamically significant stenosis when using best cut-off values

	TP/FP/TN/FN	Sensitivity % [95%CI]	Specificity % [95%CI]	PPV % [95%CI]	NPV % [95%CI]	Accuracy % [95%CI]
MLD (mm)	69/64/64/11	86.2 [77.0–93.0]	50.0 [41.0–59.0]	51.9 [43.0–60.0]	85.3 [77.0–93.0]	49.5 [43.0–56.0]
MLA (mm^2)	67/61/67/13	83.7 [74.0–91.0]	52.3 [43.0–61.0]	52.3 [44.0–61.0]	83.8 [76.0–92.0]	64.4 [58.0–71.0]
Diameter stenosis (%)	65/43/85/15	81.2 [71.0–89.0]	66.4 [58.0–75.0]	60.2 [49.0–71.0]	85.0 [79.0–91.0]	72.1 [66.0–78.0]
Area stenosis (%)	64/49/81/14	80.0 [79.0–88.0]	63.3 [54.0–72.0]	56.6 [46.0–65.0]	88.0 [81.0–95.0]	69.7 [63.0–76.0]
Plaque burden (%)	79/25/69/35	76.2 [65.0–85.0]	66.4 [58.0–75.0]	76.0 [67.0–85.0]	66.3 [72.0–86.0]	72.2 [66.0–78.0]
Lesion length (mm)	39/20/107/42	48.7 [37.0–60.0]	83.6 [76.0–90.0]	66.1 [56.0–76.0]	71.8 [64.0–80.0]	70.2 [64.0–76.0]
V_{sub} (ml)	51/32/95/30	63.7 [52.0–74.0]	74.4 [66.0–82.0]	61.4 [51.0–72.0]	76.0 [69.0–83.0]	70.2 [64.0–76.0]
V_{ratio} (%)	61/37/91/19	76.2 [65.0–85.0]	71.1 [62.0–79.0]	62.2 [52.0–73.0]	82.7 [76.0–89.0]	73.1 [67.0–79.0]
V_{ratio}/MLD	65/26/102/15	81.3 [73.0–90.0]	79.7 [72.0–86.0]	71.4 [62.0–81.0]	87.2 [81.0–93.0]	80.3 [75.0–86.0]
V_{ratio}/MLA	50/13/115/30	62.5 [51.0–73.0]	89.8 [83.0–95.0]	79.4 [71.0–88.0]	79.3 [72.0–86.0]	79.3 [76.0–85.0]
LL/MLD^4	61/37/92/18	76.2 [65.0–85.0]	71.9 [63.0–80.0]	62.2 [53.0–72.0]	83.6 [77.0–91.0]	73.6 [68.0–80.0]
FFR_{CT}	65/21/107/15	81.2 [71.0–89.0]	83.6 [76.0–90.0]	75.6 [66.0–85.0]	87.7 [82.0–93.0]	82.7 [78.0–88.0]
FFR_{CT} + V_{ratio}/MLD	75/24/105/4	93.7 [86.0–97.9]	82.0 [74.0–88.0]	75.8 [66.0–85.0]	96.3 [93.0–100.0]	86.5 [82.0–91.0]
FFR_{CT} + V_{ratio}/MLA	67/18/110/13	83.7 [74.0–91.0]	85.9 [79.0–91.0]	78.8 [70.0–88.0]	89.4 [84.0–95.0]	85.1 [80.0–90.0]
FFR_{CT} + LL/MLD^4	65/17/111/15	81.2 [71.0–89.0]	86.7 [80.0–92.0]	79.3 [71.0–88.0]	88.1 [82.0–94.0]	84.6 [80.0–90.0]
Stepwise approach*	61/7/121/19	76.3 [67.0–86.0]	94.5 [91.0–98.0]	89.7 [82.0–97.0]	86.4 [81.0–92.0]	90.9 [87.0–95.0]

CCTA, coronary computed tomography angiography; *CI*, confidence interval; *FFR*, fractional flow reserve; *LL*, lesion length; *MLA*, minimal lumen area; *MLD*, minimal lumen diameter; V_{sub}, volume of subtended myocardial mass; V_{ratio}, percentage of subtended myocardial mass

*A stepwise approach based on CT-FFR with restrictive use of V_{ratio}/MLD was designed. Lesions with CT-FFR values within 0.7 to 0.8 were reclassified according to the results of V_{ratio}/MLD

Table 5 Diagnostic performance of FFR_{CT} and V_{ratio} / MLD according to FFR_{CT} range

FFR_{CT} range	FFR_{CT} diagnostic accuracy	V_{ratio}/MLD diagnostic accuracy	*p*
≥ 0.9	91.9% (57/62)	82.3% (51/62)	0.1796
0.80–0.89	86.2% (50/58)	82.8% (48/58)	1.000
0.7–0.79	61.8% (34/55)	80.0% (44/55)	0.0001
≤ 0.69	93.9% (31/33)	72.7% (24/33)	0.2188

FFR, fractional flow reserve; *MLD*, minimal lumen diameter; V_{ratio}, percentage of subtended myocardial mass

of the Voronoi algorithm [31]: a voxel in the LV myocardium is linked to the nearest voxel on the coronary artery as its own territory. The accuracy of this approach regarding automatic myocardium segmentation has been validated by a recent animal study [14], with an excellent correlation of CT-derived myocardial volume to actual myocardial volume. Therefore, it is technically feasible to perform non-invasive myocardium quantification based on CT modality.

There are some limitations in our study. First, the retrospective design might lead to inclusion bias. Since FFR_{ICA} measurement was rarely used for the assessment of mild coronary stenosis (stenotic extent < 50%) in our hospital, the current analysis did not include mild lesions. Therefore, the diagnostic performance of ML-based FFR_{CT} and subtended myocardial mas still needs to be validated in patients with mild stenosis. Second, CFD-based FFR_{CT} was not used in the current investigation. Although previous studies showed a comparable performance of both two FFR_{CT} approaches [32, 33], whether CFD-based FFR_{CT} would result in similar results remains to be determined. Third, the present study only included a small fraction of patients who underwent CCTA in our institute. This is also a severe inclusion bias due to the retrospective nature of the study. Fourth, various other CT-based techniques or parameters have been recently reported to be able to accurately predict ischemic coronary stenosis [34–37]. Future head-to-head comparison studies are needed to determine the best method among current and those approaches. Finally, the relatively small sample size might also partially lead to the discrepant finding regarding the relationship between plaque characteristics and hemodynamic significance. For these reasons, future prospective studies with larger sample size are required to confirm the current finding.

In conclusion, ML-based FFR_{CT} simulation and V_{ratio}/MLD both performed well for predicting hemodynamic status. V_{ratio}/MLD was more accurate than ML-based FFR_{CT} for lesions with simulated FFR value ranging from 0.7 to 0.8. However, the high-risk plaque features failed to show a significant correlation with the hemodynamic significance.

Funding This study has received funding from the National Natural Science Foundation of China (Grant No.: 81671678), Shanghai Municipal Education Commission-Gaofeng Clinical Medicine Grant Support (Grant No.: 20161428), Shanghai Key Discipline of Medical Imaging (No.: 2017ZZ02005), and The National Key Research and Development Program of China (Grant Nos.: 2016YFC1300400 and 2016YFC1300402).

Compliance with ethical standards

Guarantor The scientific guarantor of this publication is Dr. Jiayin Zhang.

Conflict of interest The authors of this manuscript declare no relationships with any companies, whose products or services may be related to the subject matter of the article.

Statistics and biometry No complex statistical methods were necessary for this paper.

Informed consent Written informed consent was waived by hospital IRB.

Ethical approval Institutional Review Board approval was obtained.

Methodology
- retrospective
- comparative study
- performed at one institution

References

1. Miller JM, Rochitte CE, Dewey M et al (2008) Diagnostic performance of coronary angiography by 64-row CT. N Engl J Med 359(22):2324–2336
2. Westwood ME, Raatz HD, Misso K et al (2013) Systematic review of the accuracy of dual-source cardiac CT for detection of arterial stenosis in difficult to image patient groups. Radiology 267(2):387–395
3. Yang L, Zhou T, Zhang R et al (2014) Meta-analysis: diagnostic accuracy of coronary CT angiography with prospective ECG gating based on step-and-shoot, flash and volume modes for detection of coronary artery disease. Eur Radiol 24(10):2345–2352
4. Toth G, Hamilos M, Pyxaras S et al (2014) Evolving concepts of angiogram: fractional flow reserve discordances in 4000 coronary stenoses. Eur Heart J 35(40):2831–2838
5. Tonino PA, Fearon WF, De Bruyne B et al (2010) Angiographic versus functional severity of coronary artery stenoses in the FAME study fractional flow reserve versus angiography in multivessel evaluation. J Am Coll Cardiol 55(25):2816–2821
6. Taylor CA, Fonte TA, Min JK (2013) Computational fluid dynamics applied to cardiac computed tomography for noninvasive quantification of fractional flow reserve: scientific basis. J Am Coll Cardiol 61(22):2233–2241
7. Nørgaard BL, Leipsic J, Gaur S et al (2014) Diagnostic performance of noninvasive fractional flow reserve derived from coronary computed tomography angiography in suspected coronary artery disease: the NXT trial (analysis of coronary blood flow using CT angiography: next steps). J Am Coll Cardiol 63(12):1145–1155
8. Min JK, Leipsic J, Pencina MJ et al (2012) Diagnostic accuracy of fractional flow reserve from anatomic CT angiography. JAMA 308:1237–1245

9. Itu L, Rapaka S, Passerini T et al (2016) A machine-learning approach for computation of fractional flow reserve from coronary computed tomography. J Appl Physiol (1985) 121(1):42–52
10. Park HB, Heo R, ó Hartaigh B et al (2015) Atherosclerotic plaque characteristics by CT angiography identify coronary lesions that cause ischemia: a direct comparison to fractional flow reserve. JACC Cardiovasc Imaging 8(1):1–10
11. Driessen RS, Stuijfzand WJ, Raijmakers PG et al (2018) Effect of plaque burden and morphology on myocardial blood flow and fractional flow reserve. J Am Coll Cardiol 71(5):499–509
12. Califf RM, Phillips HR 3rd, Hindman MC et al (1985) Prognostic value of a coronary artery jeopardy score. J Am Coll Cardiol 5(5): 1055–1063
13. Yu M, Zhao Y, Li W et al (2018) Relationship of the Duke jeopardy score combined with minimal lumen diameter as assessed by computed tomography angiography to the hemodynamic relevance of coronary artery stenosis. J Cardiovasc Comput Tomogr 12(3):247–254
14. Ide S, Sumitsuji S, Yamaguchi O, Sakata Y (2017) Cardiac computed tomography-derived myocardial mass at risk using the Voronoi-based segmentation algorithm: a histological validation study. J Cardiovasc Comput Tomogr 11(3):179–182
15. Min JK, Shaw LJ, Devereux RB et al (2007) Prognostic value of multidetector coronary computed tomographic angiography for prediction of all-cause mortality. J Am Coll Cardiol 50:1161–1170
16. Yu M, Lu Z, Li W, Wei M, Yan J, Zhang J (2018) CT morphological index provides incremental value to machine learning based CT-FFR for predicting hemodynamically significant coronary stenosis. Int J Cardiol 265:256–261
17. Pijls NH, De Bruyne B, Peels K et al (1996) Measurement of fractional flow reserve to assess the functional severity of coronary-artery stenoses. N Engl J Med 334(26):1703–1708
18. DeLong ER, DeLong DM, Clarke-Pearson DL (1988) Comparing the areas under two or more correlated receiver operating characteristic curves: a nonparametric approach. Biometrics 44(3):837–845
19. Cook CM, Petraco R, Shun-Shin MJ et al (2017) Diagnostic accuracy of computed tomography-derived fractional flow reserve: a systematic review. JAMA Cardiol 2(7):803–810
20. Tonino PA, De Bruyne B, Pijls NH et al (2009) Fractional flow reserve versus angiography for guiding percutaneous coronary intervention. N Engl J Med 360(3):213–224
21. De Bruyne B, Pijls NH, Kalesan B et al (2012) Fractional flow reserve-guided PCI versus medical therapy in stable coronary disease. N Engl J Med 367(11):991–1001
22. De Bruyne B, Fearon WF, Pijls NH et al (2014) Fractional flow reserve-guided PCI for stable coronary artery disease. N Engl J Med 371(13):1208–1217
23. Leone AM, De Caterina AR, Basile E et al (2013) Influence of the amount of myocardium subtended by a stenosis on fractional flow reserve. Circ Cardiovasc Interv 6(1):29–36
24. Ahmadi A, Stone GW, Leipsic J et al (2016) Association of coronary stenosis and plaque morphology with fractional flow reserve and outcomes. JAMA Cardiol 1(3):350–357
25. Gaur S, Øvrehus KA, Dey D et al (2016) Coronary plaque quantification and fractional flow reserve by coronary computed tomography angiography identify ischaemia-causing lesions. Eur Heart J 13:1220–1227
26. Waksman R, Legutko J, Singh J et al (2013) FIRST: Fractional Flow Reserve and Intravascular Ultrasound Relationship Study. J Am Coll Cardiol 61:917–923
27. Brugaletta S, Garcia-Garcia HM, Shen ZJ et al (2012) Morphology of coronary artery lesions assessed by virtual histology intravascular ultrasound tissue characterization and fractional flow reserve. Int J Cardiovasc Imaging 28:221–228
28. Yu M, Lu Z, Li W et al (2018) Coronary plaque characteristics on baseline CT predict the need for late revascularization in symptomatic patients after percutaneous intervention. Eur Radiol 28(8): 3441–3453
29. Yu M, Li W, Lu Z et al (2018) Quantitative baseline CT plaque characterization of unrevascularized non-culprit intermediate coronary stenosis predicts lesion volume progression and long-term prognosis: a serial CT follow-up study. Int J Cardiol 264:181–186
30. Ferencik M, Mayrhofer T, Bittner DO et al (2018) Use of high-risk coronary atherosclerotic plaque detection for risk stratification of patients with stable chest pain: a secondary analysis of the PROMISE randomized clinical trial. JAMA Cardiol 3(2):144–152
31. Guibas L, Stolfi J (1985) Primitives for the manipulation of general subdivisions and the computations of Voronoi diagrams. ACM Trans Graph 4:74–123
32. Tesche C, De Cecco CN, Baumann S et al (2018) Coronary CT angiography-derived fractional flow reserve: machine learning algorithm versus computational fluid dynamics modeling. Radiology 288(1):64–72
33. Coenen A, Kim YH, Kruk M et al (2018) Diagnostic accuracy of a machine-learning approach to coronary computed tomographic angiography-based fractional flow reserve: result from the MACHINE consortium. Circ Cardiovasc Imaging 11(6):e007217
34. Dey D, Gaur S, Ovrehus KA et al (2018) Integrated prediction of lesion-specific ischaemia from quantitative coronary CT angiography using machine learning: a multicentre study. Eur Radiol 28(6): 2655–2664
35. von Knebel Doeberitz PL, De Cecco CN, Schoepf UJ et al (2018) Coronary CT angiography-derived plaque quantification with artificial intelligence CT fractional flow reserve for the identification of lesion-specific ischemia. Eur Radiol. https://doi.org/10.1007/s00330-018-5834-z
36. Siogkas PK, Anagnostopoulos CD, Liga R et al (2018) Noninvasive CT-based hemodynamic assessment of coronary lesions derived from fast computational analysis: a comparison against fractional flow reserve. Eur Radiol. https://doi.org/10.1007/s00330-018-5781-8
37. van Hamersvelt RW, Zreik M, Voskuil M, Viergever MA, Išgum I, Leiner T (2018) Deep learning analysis of left ventricular myocardium in CT angiographic intermediate-degree coronary stenosis improves the diagnostic accuracy for identification of functionally significant stenosis. Eur Radiol. https://doi.org/10.1007/s00330-018-5822-3